Rock Mechanics Contributions and Challenges, Hustrulid & Johnson (eds)
© 1990 Balkema, Rotterdam. ISBN 90 6191 123 0

Microseismic source locations: A test of faith

L.H. Estey, P.L. Swanson, F.M. Boler & S. Billington
Bureau of Mines, Denver Research Center, Denver, Colo.

1 INTRODUCTION

High-resolution locations of microseismic events in mines would greatly augment the identification and mapping of geologic structures such as faults within the rock mass. Monitoring the movement and stress in the rock mass within the mining environment by microseismic analysis should aid in the understanding of rock bursting. Such monitoring by focal mechanism analysis is critically dependent upon high-resolution locations *and* accurate knowledge of the three-dimensional seismic velocity structure within the rock mass (Billington et al. 1990).

The Bureau of Mines is developing methods for such quantitative characterization of deformation by studying a working hard-rock mine located in the Coeur D'Alene district of northern Idaho which has discontinuous geologic structure. Routine locations of microseismic events in the mine at different stopes, based on arrival times of P-waves at different receivers, have been used to identify those stopes with a higher probability of bump or burst activity. Adding to this analysis by correlating individual events with known geologic structures, identifying and mapping unknown structures within the rock mass, and determining the direct causes of fracturing will require microseismic locations with high accuracy and precision. As a result, a current research direction is the identification of those parameters and/or numerical procedures which affect the computed location of a given microseismic event. The parameters considered here are the receiver coordinates, arrival time picks, and velocity field model. Numerical procedures include the location technique (i.e., basis function and numerical algorithm) and associated procedures such as receiver weighting, arrival weighting, and screening procedures.

2 NUMERICAL LOCATION TECHNIQUES

Two general classes of numerical location techniques were considered: direct solution and iterative solution. Direct solution techniques are derived by taking differences between the squares of the travel-time equation for different receivers and finding a simplification which is linear in the source coordinates (which may or may not include the source origin time). Hence, a single inversion of a set of these direct equations suffices to locate the source. Two different direct solution techniques were examined. One is a generalized form of the technique

derived independently by Salamon & Wiebols (1974: 158, equation 71) and by Godson et al. (1980: 157, equation 7) which will here be called the SW-GBM basis function. Salamon and Wiebols cast their function in terms of the origin time of the source, whereas Godson et al. cast their function in terms of the arrival time at the first hit receiver; however, either one can easily be converted into the other. In generalized form, the SW-GBM basis results in m(m-1)/2 equations for m receivers with an arrival of the same seismic phase, of which m-1 independent equations can be selected. Both Salamon and Wiebols and Godson et al. suggested subsets of m-1 equations rather than the m(m-1)/2 equations, and these subsets are different from one another. The other direct solution technique was a generalized form of that derived by Blake et al. (1974: 39, equation C-11) which will here be called the BLD basis function. In generalized form, the BLD basis results in m(m-1)(m-2)/2 equations for m receivers. Thus the set of m-2 equations suggested by Blake et al. for the source location is a subset. Both the SW-GBM and BLD direct basis techniques are generally only practical for homogeneous and isotropic velocity structure--an assumption which is commonly made for the mining environment.

Iterative solution techniques are widely used for heterogeneous and/or anisotropic velocity structures. The most common approach is the gradient technique (Press et al. 1986: section 14.4). An initial starting solution is assumed, and a correction to this solution is then found and added to the solution, with the process repeating iteratively until the correction is sufficiently small or some other stopping criterion is met. For the location problem, the form of the equation for the correction (i.e., the gradient) is linear in source coordinates. Some form of a gradient basis is usually used in broad application seismological location codes; for example, a type of full-gradient basis (source location and origin time) is used in HYPOINVERSE (Klein 1978) and a spatial-gradient basis (source location only) is used in HYPO71 (Lee & Lahr 1972) and HYPOCENTER (Lienert et al. 1986). For both of these gradient bases, there are m independent equations which are formed and solved iteratively for m receivers.

The four linear basis functions above were selected for study, i.e., the two generalized direct bases (SW-GBM and BLD) and the two gradient bases (full and spatial). Some general numerical algorithm for solving the simultaneous systems of equations formed by these bases is desired. The resulting systems of equations are generally overdetermined (i.e., the number of equations is larger than the number of unknowns). Forming the normal equations for an overdetermined system is undesirable from a numerical analysis standpoint, since this operation squares the condition number of the system to be solved (e.g., Dahlquist & Björck 1974: section 5.7.1 or Press et al. 1986: section 14.3; and Niewiadomski 1989); therefore, numerical algorithms such as Choleski decomposition were not used. Two L_2 residual norm minimization (i.e., least-squares) algorithms which are applicable for overdetermined systems were tested; these are the QR-decomposition and singular value decomposition (SVD) (see e.g., Dahlquist and Björck, Press et al.) which can be coded to directly solve overdetermined systems without forming the normal equations. The code for the QR algorithm was written by the first author; the code for the SVD algorithm was adapted from Fortran code given in Press et al. These QR and SVD codes gave nearly identical results, which is not surprising since the SVD algorithm is based on a QR decomposition (e.g., Press et al., section 2.9). Solutions using the somewhat more involved SVD codes are useful if one wishes to obtain an error estimate of the solution (assuming all errors are normally

distributed). A linear simplex algorithm should give an L_1 residual norm minimization and, as a result, should be less sensitive to outlying data points than least-squares algorithms. However, trial solutions made by using a linear simplex code gave erratic results. The results discussed below implemented either a QR-decomposition or SVD code to solve the linear systems formed by the four basis functions.

In the absence of error, all numerical location techniques should be able to locate sources very well, that is, the difference between a true (synthetic) source location and the final result of the location technique should be due to numerical noise of both the input data and the numerical algorithms used. For the size of the typical array in the mine under study (~100 m across) and the particular hardware being used (32-bit single-precision floating point), these numerical errors amount to discrepancies between a synthetic source and the computed location of this synthetic source of at most a few centimeters, with typical discrepancies of millimeters or less. This was found to be true regardless of what basis was used for the location process.

3 PHYSICAL SOURCES OF ERROR

Next, an attempt was made to model the various physical errors associated with a real microseismic array assuming a simple homogeneous and isotropic velocity structure. One source of error is the spatial uncertainty of the receiver coordinates. Receiver positions for a real array were obtained by a survey using electronic distance measurement (EDM) equipment. The uncertainties associated with the EDM-surveyed receiver coordinates are estimated to be 0.05 m or less.

Another source of error is the temporal uncertainty of the arrival time pick at each receiver. Digital waveforms of microseismic events were recorded at 100 kHz sampling with 12-bit dynamic range and were later analyzed to obtain arrival times by a person using a high-resolution graphics workstation--an interactive system discussed in detail elsewhere. These manual picks are unlikely to be earlier than the actual arrival (which is unknown) by more than one or two digitizing intervals, but could be later than the actual arrival by an amount roughly proportional to the distance of the source from the receiver. For example, impulsive arrivals were generally recorded at receivers close to the source and could often be picked with an uncertainty judged to be $\pm 10\ \mu s$, i.e., plus or minus one digitizing interval. For receivers with later arrivals (receivers farther from the source), the arrival was sometimes more emergent, probably due to attenuation of high frequencies and multi-pathing; manual P-wave picks are therefore estimated to be as much as $200\ \mu s$ late for receivers up to 200 m distant from the source for smaller events.

A third source of error is in the determination of velocity. The actual velocity structure in the typical hard-rock mine environment is complicated, due to both the geology (bedding, fault structure, ore veins, etc.) and the mining process (mine openings, sand-filled stopes, mining-induced fractures, etc.). It is reasonable to ask whether a single value for the P-velocity is in any way representative of the actual structure. Using the array discussed above, waveforms were recorded from a set of calibration blasts detonated at a surveyed site near the center of the array at a stope being worked. Using manual picks of first arrivals from the blasts and the surveyed locations of both the receivers and the blast site, an estimate of the straight-line average velocities was obtained (Figure 1a) along with the level of

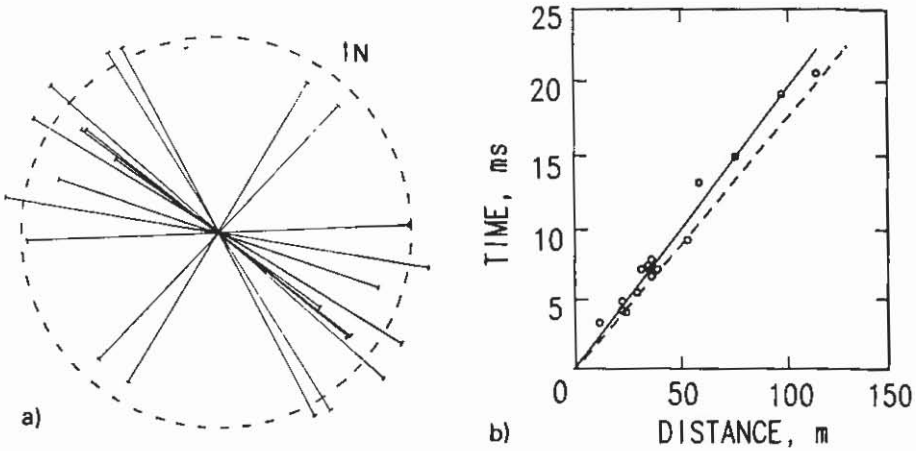

Figure 1. (a) Azimuthal variation of mean P-velocity determined from calibration blast, with dashed line representing the best fit of 5.02 km/s. (b) Travel-time vs. straight-line distance between blast site and receivers. Solid line, 5.02 km/s. Dashed line (5.64 km/s) is perhaps more typical of unfractured rock in the mine.

P-velocity heterogeneity (about ±25%) at the research site. A travel-time vs. distance analysis (Figure 1b) revealed that the mean velocity was 5.02 km/s (solid line) with an uncertainty of ±0.2 km/s with 95% confidence. A higher velocity of 5.64 km/s (dashed line) may be representative of mine-wide paths through nearly intact rock, whereas the lower velocity (5.02±0.2 km/s) may correspond to average paths near the mine openings which sample highly fractured rock.

4 RESPONSE OF NUMERICAL LOCATION TECHNIQUES TO ERROR

The influence of the physical sources of errors on the numerical location process was examined by numerical experiment. A set of 1,000 synthetic source locations were randomly chosen centered about the coordinates of the real array. Synthetic arrival times at array receivers were calculated assuming perfectly known receiver coordinates and a velocity of 5.0 km/s. Computed locations of these 1,000 synthetic events were determined after including various errors, e.g., travel time errors and receiver coordinate errors as outlined above and/or a velocity different than 5.0 km/s. The discussion of the results given below is qualitative due to space limitations; a more quantitative summary is being prepared by the authors.

It was found that solutions based on different basis functions handled errors differently. In particular, if only arrival time errors and/or receiver coordinate errors (which are largely random) were present, then the gradient bases performed better than the direct bases. (Here a basis which yielded computed locations closer to the true synthetic source sites than another basis with the same parameters was deemed to have a better location performance.) Also, the spatial-gradient basis performed slightly better than the full-gradient basis; the SW-GBM direct basis performed better than the BLD direct basis. For the direct bases, the more complete the subset of equations and the more balanced the representation of information from all receivers, the better these

bases performed. The spatial-gradient basis tended to give solutions with the lowest travel-time residuals.

However, when using a velocity different than 5.0 km/s (a strong systematic error), the best performance was obtained by using a particular subset of the SW-GBM basis functions, i.e., a subset of m-1 equations formed by pairs of receivers ordered by arrival times, which is the subset suggested by Godson et al. (1980). This was followed in performance by the BLD basis and then the gradient bases. Even though the gradient bases yielded the biggest location discrepancies in this case, the spatial-gradient basis again tended to give solutions with the lowest travel-time residuals (i.e., difference of observed and calculated arrival times).

The SW-GBM basis (with the special subset of m-1 equations) performs the best with a systematic error in velocity and does reasonably well with random errors in arrival time picks and receiver coordinates. Consequently, with the assumption of a spatially uniform velocity, this direct linear system solved by either QR-decomposition or SVD has been selected as the preferred location technique for the remainder of this investigation. However, with a more spatially complicated velocity structure, the direct basis may prove to be impractical to implement.

Location discrepancies were found for 1,000 synthetic event sites using errors typical of the above microseismic system, i.e., EDM-surveyed receiver coordinates, manual picks of first arrivals, both receiver and arrival weighting, receiver dropout (on average, one-third of 12 receivers), and the above implementation of the SW-GBM basis. Figure 2 shows the horizontal spatial discrepancies between the known synthetic source sites and the computed source sites for this system. A P-velocity of 5.2 km/s (4% error) was used for the computed locations representing a 2σ deviation in velocity from the mean of Figure 1b, whereas 5.0 km/s was used to calculate the original synthetic arrival times. The spatial discrepancies are similar in magnitude to those in Figure 2 when a P-velocity of 4.8 km/s is used for the computed locations. The vertical spatial discrepancies are about two times larger than the horizontal due to the gross receiver array geometry.

5 LOCATIONS OF CALIBRATION BLASTS

The accuracy and precision of source locations for a given system can be field tested by locating calibration blasts. In Figure 3, the computed locations of the set of five blasts used for Figure 1 are compared to the surveyed site from which all five of the blasts were detonated. The computed blast locations are at the center of skewed triad symbols which denote the axes of the spatial uncertainty ellipsoids of 95% confidence of each location using an SVD algorithm on m-1 SW-GBM basis functions.

Several observations can be made: (1) The 95% confidence error ellipsoids of the computed locations do not enclose the surveyed blast site. There is about a 10-m offset of the center of computed blast locations from the surveyed blast site. Based on the controlled-error analysis (Figure 2), errors anticipated with this microseismic system are considerably less than this amount (Figure 3). Presumably, this lack of location accuracy is due to inadequate modeling of the complex velocity structure. (2) Four of the locations form a cluster about 2 m across, and each one is contained within the 95% confidence limits of the others. Each of these four blasts had usable arrivals on about the same set of receivers; therefore, the only difference in these four blast locations comes from slightly different arrival time picks. (3) The

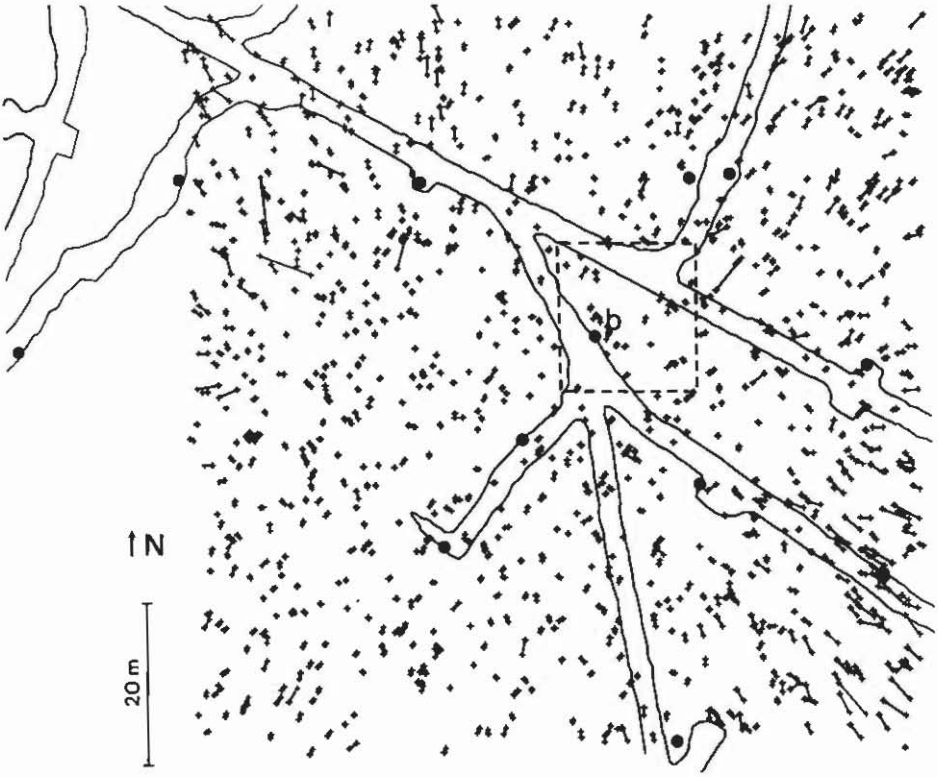

Figure 2. Plan view of mine opening geometry, receiver array (solid circles), and composite location discrepancies for 1,000 synthetic event sites using errors typical of the microseismic system discussed in the text. Surveyed position of the blast site is indicated by a "b", surrounded by a dashed box equivalent to region in Figure 3a.

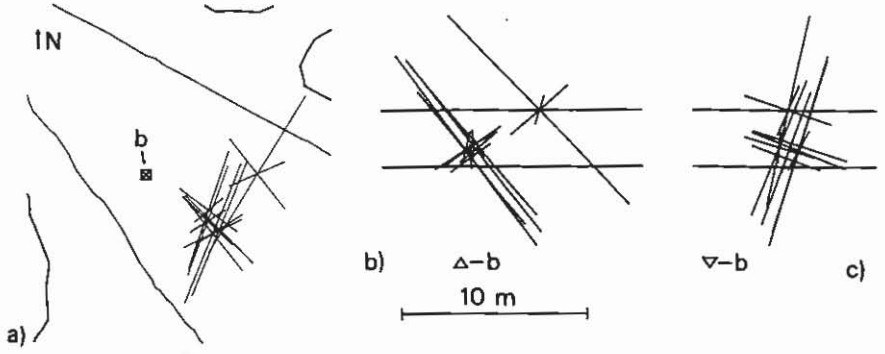

Figure 3. Computed locations of same five calibration blasts (center of skewed triad symbols) as used in Figure 1 as compared to surveyed site of all five blasts (symbol at "b") about 5 m below main level. Triad symbols indicate axes of spatial uncertainty ellipsoid at 95% confidence as determined by an SVD algorithm. (a) Plan view. (b) Vertical projection, looking NW. (c) Vertical projection, looking NE. All to same scale.

fifth blast location, which is offset from the other four, had usable arrivals on a smaller set of receivers, but had the same magnitude of relative arrival time offsets. The location offset of this fifth blast is then due primarily to array geometry effects in the numerical location process. (4) The error ellipsoids of all of the blast locations have the same general magnitude, aspect ratio, and spatial orientation. The ellipsoid magnitude scales in proportion to the mean travel-time residual of the location; the aspect ratio and the orientation is an array geometry effect. Since one of the blasts, i.e., (3) above, uses a subset of receivers from the other four, it seems that in this example the computed location of the blasts is more sensitive to the numerical location process than the SVD uncertainty of the computed location which assumes *a priori* normally distributed errors.

6 CONCLUSIONS

From a set of widely used numerical location techniques, one was found to have the lowest spatial discrepancies for synthetic events in the presence of errors using a spatially uniform velocity and m receivers. This technique uses a direct solution basis function which is used to set up m-1 independent linear equations similar to those used by Godson et al. (1980). Accounting for all errors except the actual heterogeneous velocity structure (partially indicated in Figure 1) for an array about 100 m in size results in spatial mislocation errors (Figure 2) which are comparable to the location precision of a set of calibration test blasts (Figure 3). Location precision of blasts and microseismic events for this array is probably about ±1 meter, currently limited by the ability to pick first arrivals. Location accuracy, however, is currently limited by inadequate modeling of the velocity structure rather than by receiver position accuracy. If the velocity in the mine environment were actually spatially uniform, its accurate determination would be relatively simple. The computed locations of test blasts show that (1) the velocity at the test site is not spatially uniform; and (2) its variation does not allow computed locations of calibration blasts and presumably of microseismic events with accuracy better than about 10 meters. Such accuracies may be sufficient for routine microseismic monitoring in the mine environment, but are inadequate for detailed analyses of the deformation mechanics in these media as required by source analyses such as determination of focal mechanisms. Therefore, a detailed image of the P-velocity structure at the research site will eventually be attempted through tomographic procedures.

Acknowledgments: The authors thank ASARCO Incorporated for their long-standing cooperation with the Bureau in the field experiments at the Galena Mine, C. Sines for his invaluable field assistance, and the reviewers for their comments.

REFERENCES

Billington, S., F.M. Boler, P.L. Swanson, & L.H. Estey 1990. P-wave polarity patterns from mining-induced microseismicity in a hard-rock mine. this volume.

Blake, W., F. Leighton, & W.I. Duvall 1974. Microseismic techniques for

monitoring the behavior of rock structures. U.S. Bureau of Mines Bulletin 665.
Dahlquist, G., & Å. Björck 1974. Numerical Methods. Englewood Cliffs: Prentice-Hall. translated by N. Anderson.
Godson, R.A., M.C. Bridges, & B.M. McKavanagh 1980. A 32-channel rock noise source location system. 2nd Conf. AE/Microseis. Activity in Geol. Struct. and Mater. Clausthal:Trans Tech Publ. 117-161.
Klein, R.W. 1978. Hypocenter location program HYPOINVERSE Part I: Users guide to versions 1, 2, 3, and 4. U.S. Geol. Surv. Open-File Rept. 78-694.
Lee, W.H.K., & J.C. Lahr 1972. HYPO71: A computer program for determining hypocenter, magnitude, and first motion pattern of local earthquakes. U.S. Geol. Surv. Open-File Rept. 75-311.
Lienert, B.R., E. Berg, & L.N. Frazer 1986. HYPOCENTER: An earthquake location method using centered, scaled, and adaptively damped least squares. Bull. Seismol. Soc. Amer. 76:771-783.
Niewiadomski, J. 1989. Application of singular value decomposition method for location of seismic events in mines. Pure Appl. Geophys. Res. 129:551-570.
Press, W.H., B.P. Flannery, S.A. Teukolsky, & W. T. Vetterling 1986. Numerical Recipes: The Art of Scientific Computing, Cambridge:Cambridge University Press.
Salamon, M.D.G. & G.A. Wiebols 1974. Digital location of seismic events by an underground network of seismometers using the arrival times of compressional waves. Rock Mechanics. 6:141-166.

COLORADO SCHOOL OF MINES / GOLDEN / 18-20 JUNE 1990

Rock Mechanics Contributions and Challenges: Proceedings of the 31st U.S. Symposium

Edited by
W.A. HUSTRULID
Colorado School of Mines, Golden
G.A. JOHNSON
US Bureau of Mines, Denver

A.A. BALKEMA / ROTTERDAM / BROOKFIELD / 1990

Sponsored by:

US National Committee for Rocks Mechanics and the International Society for Rock Mechanics

Assisted by:

Colorado School of Mines
US Bureau of Mines, Denver Research Center

The texts of the various papers in this volume were set individually by typists under the supervision of each of the authors concerned.

Published by
A.A. Balkema, P.O. Box 1675, 3000 BR Rotterdam, Netherlands
A.A. Balkema Publishers, Old Post Road, Brookfield, VT 05036, USA

ISBN 90 6191 123 0

Printed in the Netherlands